

# X-ray Photoelectron Spectroscopic Studies of Cadmium and Selenite Adsorption on Aluminum Oxides

CHARALAMBOS PAPELIS\*

*Environmental Engineering and Science, Department of Civil Engineering, Stanford University, Stanford, California 94305-4020*

The sorption of cadmium(II) and selenite on two porous, high surface area aluminum oxides and a nonporous crystalline aluminum oxide ( $\alpha$ - $\text{Al}_2\text{O}_3$ , corundum) was studied by X-ray photoelectron spectroscopy (XPS). The porous adsorbents used (ALCOA types CP-5 and C-33) had different sizes and pore structure but otherwise had similar characteristics. CP-5 particles were smaller than C-33 and partly microporous; C-33 particles were mesoporous and more crystalline than the CP-5 particles. The total aqueous concentrations of cadmium(II) and selenite were  $1.0 \times 10^{-4}$  and  $1.0 \times 10^{-3}$  M, respectively. Maximum surface coverages of the porous adsorbents, as estimated by XPS, were 0.8 and 0.5 monolayers for cadmium(II) and selenite, respectively. XPS estimates of cadmium and selenite surface coverages agreed well with the hypothesis that adsorbate intraparticle diffusion followed by sorption is the predominant mechanism of cadmium and selenite uptake by porous aluminas under these experimental conditions. XPS results of cadmium and selenite sorption on corundum agreed well with expected surface coverages, based on sorption isotherm data. These results have significant implications for the fate and transport of trace elements in the environment and the remediation of wastewaters and contaminated groundwaters.

## Introduction

Sorption processes at mineral-water interfaces frequently control the fate of inorganic pollutants in the environment and the geochemical cycling of trace elements. These processes are typically subdivided into adsorption, absorption, and surface precipitation (1) based on the molecular level structure of sorption complexes at the mineral-water interface. Because the mobility and availability of trace elements is a strong function of the type of sorption complex formed, our ability to distinguish between different sorption mechanisms is essential in predicting the fate of toxic inorganics in surface waters, groundwaters, and sediments.

Sorption of trace elements on oxides has also had applications in wastewater treatment. Transition aluminas, products of the thermal transformation of aluminum hydroxides and oxyhydroxides to corundum ( $\alpha$ - $\text{Al}_2\text{O}_3$ ), in particular, have been used extensively as adsorbents for inorganic and organic compounds (2-8). From a process design perspective, large, porous adsorbents with large internal surface areas would be preferable to nonporous adsorbents because of increased sorption capacity per unit volume. The rate of ion adsorption on large, porous adsorbents however could be limited by mass transfer and specifically by intraparticle diffusion.

To evaluate the potential of porous, high surface area oxides as trace element adsorbents and to increase our understanding of inorganic ion sorption processes in porous materials, equilibrium and rate of cadmium and selenite uptake experiments on porous transition aluminas were conducted, and the results are reported elsewhere (9, 10). It has been pointed out, however, that macroscopic sorption experiments alone cannot be used to distinguish between different sorption complexes (11). Spectroscopic methods can provide specific structural information about sorbed complexes and help distinguish between different sorption mechanisms. Specifically, the agreement of rate of uptake data with a diffusion model (10) was indirect evidence of ion diffusion in the porous structure of the solid. Rate of uptake and equilibrium data alone, however, can only provide indirect evidence for a particular sorption mechanism and cannot be used to distinguish, e.g., between monolayer or sub-monolayer coverage of an adsorbent and three-dimensional precipitate formation.

X-ray photoelectron spectroscopy (XPS) is one of the most widely used surface-sensitive techniques for material characterization. During the last 20 years, it has found many applications in the study of technological and earth materials. These applications include mainly studies of oxidation states of near-surface atoms, studies of semiconductor materials and catalysts, studies of ion partitioning at the mineral-water interface, studies of mineral weathering, and studies of the atomic structure of minerals and glasses. Particular strengths of the technique are its ability to probe surface layers (5-20 atomic layers) and the ability to detect all elements except hydrogen and helium. The main disadvantage for studying aqueous sorption reactions

\* Present address: Desert Research Institute, Water Resources Center, University of Nevada System, P.O. Box 19040, Las Vegas, Nevada 89132-0040; e-mail address: lambis@snsr.unr.edu.

is that XPS is a vacuum technique, so that *in situ* studies of solid-solution interfaces are not possible.

In this study, XPS was used to determine the elemental near-surface solid composition of the porous aluminas and to distinguish cadmium and selenite intraparticle diffusion from surface precipitation (or accumulation) on the external surface of the particles by determining directly an average surface coverage of the adsorbents. The estimated thickness of the adsorbed layer could then be compared to (a) surface coverage estimates based on a surface-induced precipitation model and (b) estimates based on intraparticle diffusion followed by adsorption, resulting in more uniform coverage of the entire particle surface area, including the internal pore surface area. Because XPS is a surface-sensitive technique, only the top surface layers of the adsorbents could be examined. That is, for the porous adsorbents used in these studies, only average adsorbed layer thicknesses on the external surface of the particles could be estimated. It is likely, however, that if a precipitate were formed, it would have been formed primarily on the external surface area of the particles, and therefore, it would have been easily detected.

XPS has been used in the past to evaluate the thickness of adsorbed layers on substrates (12-14). The substrates, however, in most studies were single crystals of well-characterized nonporous materials. Estimates of surface coverages of the porous adsorbents based on analysis derived from studies of flat mineral surfaces are likely to be at best semiquantitative. As a control, therefore, cadmium and selenite surface coverages on a nonporous crystalline powder (corundum) were also estimated.

## Background

A thorough introduction to X-ray photoelectron spectroscopy (XPS) is obviously beyond the scope of this paper. A very brief introduction to XPS is given by Hochella (15). A concise overview of the technique, including history; basic theory; and some applications are given by Kelly (16). Briggs and Seah (12) give a complete coverage of the technique including instrumentation, spectral interpretation, quantification, and an extended discussion of various technological applications. A fairly basic introduction to XPS with discussion of applications in geology is given by Perry et al. (17). Hochella (18) gives a more complete overview of the technique including applications in geology, mineralogy, and geochemistry, while a substantially more theoretical treatment of the subject is presented by Brundle and Baker (19).

**Basic Theory.** When materials are exposed to X-rays energetic enough to eject electrons from inner or valence shells, the difference between the incoming photon energy and electron binding energy (BE) is converted to kinetic energy of the escaping photoelectron. XPS is a surface-sensitive technique because well-defined peaks in a spectrum originate from photoelectrons that have not undergone inelastic collisions and, therefore, must originate from the top surface layers of a solid (typically between 10 and 50 Å).

**Spectral Interpretation and Chemical Shifts.** Because every element has a unique electronic structure and the low energy X-rays used can only excite a few atomic levels from each element, elements can be identified unambiguously in most cases. Contaminants in the air and residual gases in the vacuum chamber give rise to a C 1s peak, referred to as the "adventitious carbon" peak. A chemical

shift is defined as the difference in BE between a particular line and the BE for the same line in a reference compound. The chemical shift is a function of the chemical environment of an atom. By means of chemical shifts, one can often distinguish between two different oxidation states of an element in a given sample or between different coordination environments.

**Charge Referencing.** When insulators are being analyzed, the sample is necessarily insulated from the spectrometer, and the surface is charged positively as photoelectrons are ejected from the sample. This surface charging results in observed BE shifts typically between 5 and 10 eV, the same for all core levels of the same sample. To obtain accurate BEs for insulators, the magnitude of charge shifting must be estimated. This procedure is called charge referencing and is usually accomplished by either the adventitious carbon, the gold dot, or the argon implantation method. The adventitious carbon method uses the presence of adventitious carbon on practically every sample and assigns a BE to the C 1s line. Because reported values for the adventitious C 1s line range from 284.6 to 285.2 eV, the values determined with this method may be off by as much as 0.6 eV.

**Chemical Quantification.** With XPS, one can obtain at least semiquantitative estimates of the relative abundance of the elements present on the surface of a sample. If only the ratio of two elements is needed, as is often the case in surface analysis, the relative abundance of the two elements can be estimated from the photoionization cross-section (the probability that a photon will be absorbed by an electron in a specific orbital) and the intensities of the two peaks. Theoretical photoionization cross-sections were tabulated by Scofield (20). An alternative approach, however, which may give better results, is to use empirical cross-sections derived from well-defined crystalline materials where the elements whose ratio must be determined in the unknown are present.

## Materials and Methods

Porous aluminum oxides (CP-5 and C-33) were obtained from ALCOA (Alcoa Center, PA). Synthetic corundum (0.3  $\mu\text{m}$  micropolish  $\alpha\text{-Al}_2\text{O}_3$ ) was obtained from Buehler, Ltd. (Lake Bluff, IL). The complete physical-chemical characterization of CP-5 and C-33 adsorbents was presented elsewhere (9). Corundum particles were of submicron dimensions and nonporous with BET surface area as determined by nitrogen adsorption at 77 K, 15  $\text{m}^2/\text{g}$ . A summary of adsorbent characteristics relevant to this paper is given in Table 1. For the sorption experiments, the adsorbate/adsorbent ratio was normalized with respect to specific surface area for the three adsorbents studied, so that approximately equal surface coverages would result in all three adsorbents (CP-5, C-33, and  $\alpha\text{-Al}_2\text{O}_3$ ). The experimental conditions are shown in Tables 2 and 3 for cadmium and selenite samples, respectively.

The adsorption experiments were conducted as described elsewhere (9) with the exception that the solid was equilibrated with the adsorbate at the desired pH for 2 days in the reaction vessel. At the end of the equilibration period, the solid was allowed to settle, the supernatant was siphoned out of the reactor, and the solid was then resuspended, transferred to a 250-mL freeze-drying flask, and freeze-dried using a Labconco freeze dryer. The dried oxide was mounted on an aluminum stub using colloidal graphite

TABLE 1

## Summary of Adsorbent Characterization

	CP-5	C-33	corundum
particle diameters ( $\mu\text{m}$ )			
mass mean diameter	9.1	41.5	0.3
Sauter mean diameter	8.3	34.0	
surface area, density, and porosity			
$\text{N}_2$ -BET ( $\text{m}^2/\text{g}$ )	200	110	15
micropore vol ( $\text{cm}^3$ (STP)/g)	24	0	
bulk density ( $\text{g}/\text{cm}^3$ )	0.76	0.9	
porosity (-)	0.75	0.74	
typical pore diameters ( $\text{\AA}$ )	< 20	30-100	
surface stoichiometry/crystal structure			
$\text{Al}_2\text{O}_3 \cdot x\text{H}_2\text{O}$ , $x =$	0.5	0.1	0
crystal structure	disordered, low temp. transition aluma	poorly cryst., high temp. transition aluma	$\alpha$ - $\text{Al}_2\text{O}_3$ corundum

TABLE 2

## Summary of Experimental Conditions: Cadmium XPS Samples

solid	concn (M)	uptake (%)	pH	surface coverage	
				(% monolayer)	( $\mu\text{M}/\text{m}^2$ )
CP-5	$1.0 \times 10^{-4}$	100	9.0	10.0	1.2
C-33	$1.0 \times 10^{-4}$	100	9.1	10.1	1.2
$\alpha$ - $\text{Al}_2\text{O}_3$	$1.0 \times 10^{-4}$	69	8.6	6.9	0.8

TABLE 3

## Summary of Experimental Conditions: Selenite XPS Samples

solid	concn (M)	uptake (%)	pH	surface coverage	
				(% monolayer)	( $\mu\text{M}/\text{m}^2$ )
CP-5	$1.0 \times 10^{-3}$	39	5.5	39.1	4.6
C-33	$1.0 \times 10^{-3}$	19	5.5	19.6	2.2
$\alpha$ - $\text{Al}_2\text{O}_3$	$1.0 \times 10^{-3}$	26	5.0	26.2	3.1

("dag") and further dried in a 90 °C oven for 2 h before it was put in vacuum.

All XPS spectra were collected on a VG Escalab Mk II system. Instrument vacuum was typically in the upper  $10^{-9}$  mbar range. Nonmonochromatic Al  $K_{\alpha}$  X-rays ( $h\nu = 1487$  eV) were used with a constant analyzer pass energy of 50 eV for both survey and narrow scans. Step sizes 1.0 and 0.1 eV were used for survey and narrow scans, respectively. No surface charge neutralization with an electron flood gun was attempted. Charge referencing for each sample was made by the adventitious carbon method (21, 22) assuming the energy of the C 1s line to be 284.6 eV. All samples were analyzed in the same position with respect to the X-ray gun and analyzer and the position was further optimized to increase the signal of the Al 2p line.

## Results and Discussion

**Binding Energies.** Aluminum and oxygen BEs for the aluminum oxides of interest were measured on powders that were otherwise not treated except for drying at 90 °C for 2 h. In addition to the two porous adsorbents (CP-5 and C-33), two crystalline, nonporous, synthetic minerals, corundum ( $\alpha$ - $\text{Al}_2\text{O}_3$ ) and gibbsite ( $\gamma$ - $\text{Al}(\text{OH})_3$ ), were also analyzed. Aluminas and particularly  $\gamma$ - $\text{Al}_2\text{O}_3$  have been studied extensively with XPS because of their importance as catalysts and catalyst supports (23-34). The BEs of Al

2p and O 1s lines have been reported in the literature for several aluminum oxides and hydroxides (24, 25, 27-33, 35-48). Representative values are reported by Moulder et al. (49).

The Al 2p BE for all samples analyzed was the same within the accuracy of the method (73.5-73.6 eV). The porous adsorbents were "corundum-like" oxides so that the similarity in BE should not be surprising. Even in gibbsite, a hydroxide, no chemical shift was observed. Although the structural environments in aluminum oxides and hydroxides are different, the first coordination shell in both aluminum oxides and hydroxides consists of six oxygens. The effect of protons in the second coordination shell of the hydroxides apparently has a secondary effect on Al core level binding energies. The measured Al 2p BEs were in fair agreement with reported values for corundum and gibbsite. Small differences may be attributed to the charge referencing technique. As mentioned above, BEs based on the adventitious carbon charge referencing method can be in error by as much as 0.6 eV. If the values reported in the literature include charge referencing uncertainties of 0.6 eV, the total uncertainty because of charge referencing could exceed 1.0 eV. The BEs for the O 1s line for the porous adsorbents and corundum were essentially the same, 530.5 eV. The O 1s line was slightly higher for gibbsite (531.2 eV). The measured BEs for corundum and gibbsite agree with previously reported values (49).

The Cd 3d BEs, corrected for surface charging, were 405.2 and 412.0 eV for the  $3d_{5/2}$  and  $3d_{3/2}$  lines, respectively. These BEs could be assigned to three possible chemical states, namely, Cd (405.1-405.0 eV), CdO (405.2 eV), or Cd(OH)<sub>2</sub> (405.0 eV) (49). On the basis of the cadmium surface coverage estimated (see below), it is highly unlikely that the observed peak corresponds to a pure Cd metal phase. In addition, the precipitation of such a phase from an aqueous cadmium solution is thermodynamically not favored. On the basis of XPS alone, we could not distinguish between the other two possible phases. In either compound, however, Cd is coordinated to O in a coordination environment similar to what is expected for Cd(II) (a metal cation) coordinated to surface hydroxyl groups of an oxide. Additional *in situ* spectroscopic evidence and specifically X-ray absorption spectroscopy (XAS) suggest the presence of mononuclear cadmium surface complexes, under these experimental conditions, with cadmium coordinated to  $6 \pm 20\%$  oxygens at  $2.33 \pm 0.01$  Å. The absence of Cd second-

nearest neighbors suggests the absence of any pure precipitated phase (50). The Cd coordination environment (Cd octahedrally coordinated by O) as determined by XAS is therefore consistent with the coordination environment suggested by XPS.

The spin orbit splitting measured, 6.8 eV, was in excellent agreement with the value reported in the literature (49) as expected because the spin orbit splitting is only weakly influenced by chemical changes. BE values are not reported for the C-33 and corundum samples because it is believed that the slightly lower BE in each successive sample was caused by sample damage and did not represent a chemical shift. The total energy shift (if totally attributed to sample damage) was approximately 1.0 eV for several hours exposure to vacuum.

The observed shift was probably not caused by an increase in contaminant concentration over time, because such changes would have been accounted for by a shift in the adventitious carbon C 1s peak. A more detailed study, however, to isolate the exact cause of BE reduction was not conducted. Although XPS is one of the least destructive techniques, reduction due to irradiation, especially of metals in higher oxidation states, has been reported (refs 17 and 51 and references cited therein). Cd(I) has been known to occur as a result of irradiation (52). Simultaneous exposure to vacuum and X-ray photons could possibly lead to slightly reduced, unusual forms of cadmium. The CP-5 sample was analyzed shortly after it was introduced in the analytic chamber, and therefore, the reported BE is considered valid.

The Se 3d BE in a sample with  $1.0 \times 10^{-3}$  M selenite sorbed on CP-5 was 58.8 eV (after charge referencing). Assuming a charge referencing uncertainty of approximately 0.6 eV, the measured BE could correspond to either  $\text{SeO}_2$  (58.9–59.8 eV),  $\text{H}_2\text{SeO}_3$  (59.2–59.9 eV), or  $\text{Na}_2\text{SeO}_3$  (59.1 eV) (49). The uncertainty in the reported values for these three Se(IV) states does not allow unambiguous assignment based on XPS-measured BEs alone. As in the case of Cd, however, additional information from XAS studies can be used to eliminate some of the possibilities. Based on *in situ* XAS measurements, Se(IV) sorbed on these aluminum oxides is coordinated by  $3.3 \pm 20\%$  O at  $1.70 \pm 0.01 \text{ \AA}$  (50), which is the coordination environment of Se(IV) in the selenite ion.  $\text{SeO}_2$ , therefore, can be ruled out as a sorbed species. Distinguishing between the remaining two possibilities (selenious acid and sodium selenite) is not important because in both compounds Se(IV) is in the coordination environment of the selenite ion, which is more likely to be the sorbing species as opposed to the undissociated form.

In addition, the BE of the Se 3d line definitely corresponds to selenite (Se(IV)) and rules out the possibility of oxidation of the adsorbate to form selenate (Se(VI)). This result is consistent with selenite equilibrium sorption and ionic strength dependence experiments (9). These types of experiments yield dramatically different results for the two oxidation states of selenium (53). As in the case of cadmium, values of BEs for selenite adsorbed on C-33 or corundum are not reported because the sample was possibly damaged by vacuum or by X-ray photons resulting in a slight reduction in BE by as much as 1.0 eV in the worst case. Such a reduction cannot be ruled out because lower oxidation states of selenium are known (52). The CP-5 sample was analyzed shortly after it was placed in vacuum, so it is believed that the damage was negligible.

#### Estimation of Surface Coverages of the Adsorbents.

XPS was used to provide estimates of cadmium or selenite surface coverages of the adsorbents. These estimates were then used to determine the most likely of the following two possible scenarios: (1) diffusion of cadmium and selenite in the pores of the transition aluminas followed by sorption or (2) surface precipitation, presumably on the external surface of the particles. Based on sorption isotherms, the total amount of cadmium or selenite sorbed was known. The distribution of the adsorbates on the surface of the particles, however, would be dramatically different depending on whether the total surface area of the particles was utilized (including internal surface area), which would imply diffusion in the pore structure of the adsorbents, or whether a precipitate was formed on the external surface of the particles.

The dramatic difference in the expected surface coverages for the two scenarios stems from the high internal surface area associated with the transition aluminas. The external equivalent sphere surface area of the transition aluminas was only a small fraction of the BET measured total surface area (approximately 0.5 and 0.2% for CP-5 and C-33, respectively; see below for external surface area calculations). As a control of this approach, surface coverages on a nonporous adsorbent, corundum ( $\alpha\text{-Al}_2\text{O}_3$ ), were also measured to estimate the accuracy of the technique. For corundum, the total amount of sorbed cadmium or selenite was known. In addition, sorbates would be located entirely at the particle surface, and therefore, they would be detected by XPS provided the surface coverage exceeded the detection limit of the technique. The comparison between expected and XPS-measured surface coverages of corundum could be used as a measure of the accuracy of this approach.

To estimate the surface coverage of the adsorbents, the intensity of the peak from the trace element of interest, cadmium or selenite, was compared to the intensity of the aluminum peak by collecting narrow scans of the Al 2p and Cd 3d (or Se 3d) regions. The areas under the Al 2p and Cd 3d peaks were integrated using the VG 5000/5250 software, following Shirley background subtraction. The area under the Se 3d peak could not be integrated directly because of the presence of the aluminum satellite. The peak was fitted using a least-squares Gaussian-Lorentzian curve-fitting routine, also using the VG 5000/5250 software.

Once the intensities of the substrate (aluminum) and adsorbate (cadmium or selenite) peaks were determined, the surface coverages were estimated as follows. The adsorbed layer thickness was first calculated using eq 1, a modification of the equation used by Hochella and Carim (13) to estimate the thickness of a  $\text{SiO}_2$  layer on a Si substrate

$$x = -\lambda_\alpha \cos \theta \ln \left( 1 - \frac{I_x / \sigma_x}{I_x / \sigma_x + I_{\text{sub}} / \sigma_{\text{sub}}} \right) \quad (1)$$

where  $x$  is the adsorbed layer thickness ( $\text{\AA}$ ),  $\lambda_\alpha$  is the attenuation length ( $\text{\AA}$ ),  $\theta$  is the angle between the sample normal and the direction of the detector,  $I_x$  and  $I_{\text{sub}}$  are the intensities of the photoelectron peaks from the adsorbed element and substrate, respectively, and  $\sigma_x$  and  $\sigma_{\text{sub}}$  are the photoionization cross-sections of the adsorbed element and substrate, respectively. The only difference between eq 1 and the original expression used by Hochella and Carim (13) is that differences in photoionization cross-sections of photoelectrons from substrate and adsorbate are significant

and must be taken into account explicitly, whereas in the original reference the cross-sections of Si 2p electrons in the Si substrate and SiO<sub>2</sub> film were assumed to be approximately equal and, therefore, not included.

Several important assumptions involved in the calculation of adsorbed layer thicknesses using eq 1 should be stated. As mentioned above, eq 1 was derived from a study of a SiO<sub>2</sub> film of uniform thickness on a silicon substrate. It was assumed that the attenuation length was essentially the same for film and substrate and that it was uniform throughout the layer. For the present study, if we assume submonolayer coverage—consistent with adsorbate intraparticle diffusion—the film is so thin that it can probably be ignored. The assumption of uniform attenuation length throughout the layer and substrate, considering the porous structure of the particles and possibly the formation of a partial monolayer, is at best an approximation. Even the assumption of a layer exclusively located at the surface is not valid if indeed the adsorbate is diffusing in the pores of the particles. Furthermore, the angle  $\theta$  cannot be defined for powders, so it was arbitrarily set to zero. In the absence of more relevant information, the attenuation length was assumed to be 15 Å, a value used by Hochella and Carim (13). Theoretical photoionization cross-sections were used for the Al 2p, Cd 3d, and Se 3d peaks (20). If a final assumption about the thickness of a monolayer is made (1.5 Å was assumed in this study), the number of adsorbed monolayers can be estimated. This estimate is at best semiquantitative considering the assumptions stated. Calculated thicknesses of less than one monolayer were converted to equivalent partial monolayer coverages. For example, a thickness of 0.5 Å was considered equivalent to 33% monolayer coverage.

Deviations from the stated assumptions would tend to increase the uncertainties in surface coverage estimations. For example, nonuniform coverage of the surface (formation of adsorbate "island structures") may result in local surface coverages substantially higher than the average calculated by eq 1. The formation of such "island structures" cannot be ruled out based on the spatial resolution of the spectrometer used. Independent X-ray absorption spectroscopy (XAS) experiments however are consistent with the absence of surface precipitates or polynuclear species under these experimental conditions and, therefore, in agreement with more homogeneous coverage of the adsorbents (50).

The surface coverages estimated from XPS measurements were compared to estimates based on total trace element uptake and two different values of surface areas related to the two different sorption mechanisms. In both cases, a site density of 7 sites/nm<sup>2</sup> was assumed. For diffusion of the adsorbate in the particles followed by adsorption, the nitrogen-BET surface area was used for surface coverage calculations. For preferential accumulation of adsorbates (surface precipitation or polymerization) at the external surface of the particles, an estimate of the external surface area of the particles was used for surface coverage calculations. The external surface area, 1.0 and 0.2 m<sup>2</sup>/g for CP-5 and C-33, respectively, was calculated using eq 2 (54)

$$A = \frac{6}{Q_b d_{vs}} \quad (2)$$

where  $A$  is the surface area (m<sup>2</sup>/g),  $Q_b$  is the bulk density

TABLE 4

Comparison of Percent Monolayer Coverage of Aluminas As Determined by Total Cadmium Uptake and XPS<sup>a</sup>

solid	based on uptake and surface area		measd by XPS
	external	total	
CP-5	2 100	10	84
C-33	5 500	10	17
$\alpha$ -Al <sub>2</sub> O <sub>3</sub>	7	7	5

<sup>a</sup> See text for assumptions.

TABLE 5

Comparison of Percent Monolayer Coverage of Aluminas As Determined by Total Selenite Uptake and XPS<sup>a</sup>

solid	based on uptake and surface area		measd by XPS
	external	total	
CP-5	8 200	39	46
C-33	11 000	20	16
$\alpha$ -Al <sub>2</sub> O <sub>3</sub>	26	26	*

<sup>a</sup> See text for assumptions. An asterisk (\*) means not quantifiable but present.

of the solid (g/m<sup>3</sup>), and  $d_{vs}$  is the equivalent sphere diameter of the particles (Sauter mean diameter, m). The surface area estimated this way is a lower limit for the external surface area; surface roughness and fines would tend to increase the actual external surface area. The surface coverages for the two sorption mechanisms are compared to the estimates from XPS (calculated using eq 1) in Tables 4 and 5 for cadmium and selenite, respectively.

**Cadmium Surface Coverage of the Adsorbents.** The narrow scans of the Al 2p and Cd 3d regions for a sample with  $1.0 \times 10^{-4}$  M cadmium adsorbed on 0.43 g/L CP-5 are shown in Figure 1. Surface coverage estimates based on external surface area, total surface area, and from XPS were 21, 0.1, and 0.84 monolayers, respectively. Even if we accept that, because of surface roughness and pore surface area close to the surface, the readily available external surface area may be higher than estimated by eq 2 by a factor of 5–10 (a mean roughness factor of 7 was determined based on a wide range of particle sizes of unweathered minerals (55)), the resulting surface coverage would still be higher than the XPS estimate by an order of magnitude. Clearly, the hypothesis of diffusion and adsorption inside the particles agrees much better with the spectroscopic data than the assumption of surface-induced precipitation.

There are several reasons for the overestimation of surface coverage by XPS. The assumption that the adsorbed layer was located exclusively at the surface of the adsorbent, which was used to derive eq 1, does not strictly speaking apply for highly porous particles. Overestimation results from the contribution to the signal of the adsorbed element from deeper layers. If the surface coverage in the pores was 10%, superposition of the signal from several layers would result in overestimation of the surface coverage compared to the case where the same surface coverage (10%) occurred only in the top surface layer.

In a sample with  $1.0 \times 10^{-4}$  M cadmium adsorbed on 0.77 g/L C-33, the XPS-measured surface coverage estimate (0.17 monolayer) agrees well with the diffusion-limited

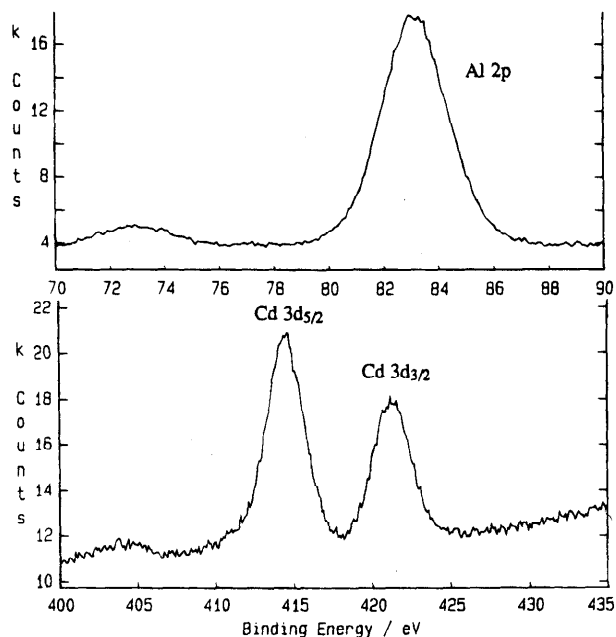


**FIGURE 1.** Comparison of Al 2p and Cd 3d X-ray photoelectron spectra from a sample with 0.1 mM cadmium adsorbed on 0.43 g/L CP-5. Surface coverage,  $1.2 \mu\text{M m}^{-2}$ .

sorption hypothesis (0.1 monolayer) and is orders of magnitude lower than the expected surface coverage based on accumulation on the external surface area (55 monolayers). The agreement is much better than for CP-5. This may be explained by the different structure of the two solids. C-33 had a coarser pore structure than CP-5 (Table 1) so that the amplification of the signal from deeper layers may not be as important a factor as for CP-5 where cadmium concentration (per volume of adsorbent) is higher.

Estimates of surface coverage from cadmium uptake and XPS for a sample with  $1.0 \times 10^{-4}$  M cadmium adsorbed on 5.7 g/L corundum are 0.07 and 0.05, respectively. The comparison of surface coverages based on the nonporous corundum sample is of special importance because contribution from deeper layers to the signal is absent and the assumptions on which eq 1 is based are more realistic. The difference between the two estimates was even smaller than for C-33, in agreement with the hypothesis that contribution to the signal from adsorbate in pores tends to inflate the surface coverage estimated from XPS. Corundum was the only sample for which the estimate based on XPS gave a slightly lower number than total metal uptake considerations. The agreement between the two estimates however is good considering the uncertainties involved in both calculations.

**Selenite Surface Coverage of the Adsorbents.** Narrow scans of the Al 2p and Se 3d regions for a sample with  $1.0 \times 10^{-3}$  M selenite adsorbed on 0.43 g/L CP-5 are shown in Figure 2. The surface coverage calculated according to eq 1 (0.46) was in very good agreement with the surface coverage based on total surface area utilization (0.39). There should be no doubt that, in light of these results, diffusion followed by adsorption is a much more reasonable assumption than surface precipitation on the external surface of the particles. The agreement was much better than with cadmium adsorbed, and if the argument made in the case of cadmium is true (namely, that selenite sorbed in pores leads to an apparently increased signal), then selenite adsorption appears to be underestimated.

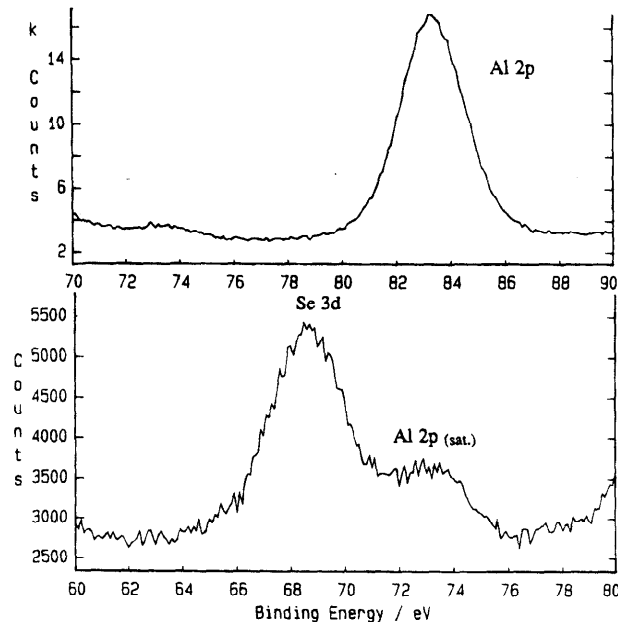


**FIGURE 2.** Comparison of Al 2p and Se 3d X-ray photoelectron spectra from a sample with 1.0 mM selenite adsorbed on 0.43 g/L CP-5. Surface coverage,  $4.6 \mu\text{M m}^{-2}$ .

There are significant differences in sensitivity of the method for Cd and Se 3d lines. The photoionization cross-sections are 2.29 for the Se 3d line and 20.22 for the Cd 3d line (20). These differences in sensitivity should not affect the surface coverage calculations however because the photoionization cross-section is included in the calculation formula (eq 1). Nevertheless, the same sorbed concentration of Cd and Se will result in peak areas substantially different. At low surface coverages, approaching the detection limit of the technique, the quantification of selenite may therefore be affected by the presence of the Al 2p satellites, which may partly mask the Se 3d peak (Se 3d BE 58.8 eV, Al 2p satellites at 63.7 (Al  $K_{\alpha 3}$ ) and 61.7 eV (Al  $K_{\alpha 4}$ )). In addition, because the attenuation length is dependent on the kinetic energy of the photoelectrons, there may be a different drop in intensity for the two elements due to (1) electron escape through the alumina matrix (for electrons originating inside pores) and (2) adventitious carbon (estimated to be about one monolayer, based on the area of the C 1s peak). These differences, however, should not affect the calculated surface coverages by a factor of more than 2.

The expected surface coverage of a sample with  $1.0 \times 10^{-3}$  M selenite adsorbed on 0.77 g/L C-33 based on the intraparticle diffusion hypothesis is 0.2 monolayer, and XPS gave an estimate of 0.16 monolayer, an excellent agreement. XPS appears to slightly underestimate the surface coverage on this solid (C-33) relative to selenite adsorption on CP-5, consistent with the trend observed for cadmium adsorption on CP-5 and C-33 (Tables 4 and 5). The same argument of different pore structure could be used to explain this trend.

The final XPS sample was a sorption sample with  $1.0 \times 10^{-3}$  M selenite adsorbed on 5.7 g/L corundum. The narrow scans of the Al 2p and Se 3d regions are shown in Figure 3. The Se 3d peak is not observable in this sample, although selenite is present on the surface as the survey scan for this sample suggests (Figure 4). The Se 3d line, even though it is the most characteristic photoelectric line of the element, is not very intense. The most intense observable line for

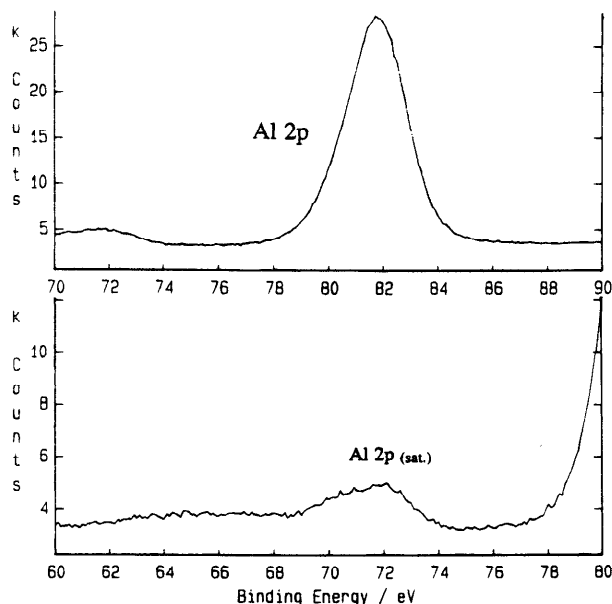


FIGURE 3. Comparison of Al 2p and Se 3d X-ray photoelectron spectra from a sample with 1.0 mM selenite adsorbed on 5.7 g/L corundum. Surface coverage,  $3.1 \mu\text{M m}^{-2}$ .

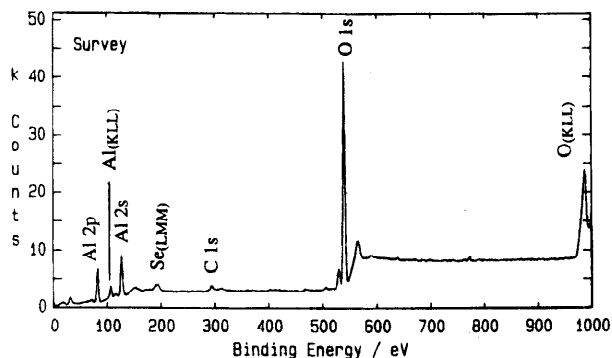


FIGURE 4. X-ray photoelectron spectrum of a sample with 1.0 mM selenite adsorbed on 5.7 g/L corundum. Compare the LMM Auger peak at approximately 190 eV with the absence of a Se 3d peak in Figure 3. Surface coverage,  $3.1 \mu\text{M m}^{-2}$ .

selenium is the Auger  $L_3M_{45}M_{45}$  line at 181 eV (with Al  $K_{\alpha}$  X-rays), and this line is clearly observable in the survey spectrum (Figure 4) at approximately 190 eV, the expected position if charge shifting of approximately 9.3 eV is taken into account. It seems unlikely that this line is due to a contaminant because it was only (and always) observed on samples that were exposed to selenite solutions. The fact that there is direct evidence for the presence of selenite on the surface but the amount cannot be quantified from the Se 3d line suggests that quantification of selenite adsorption may be underestimated, in agreement with the conclusions reached by comparing cadmium and selenite surface coverages. The fact that for similar surface coverages on two solids (C-33 and corundum) selenite is detectable on the porous solid but not on the nonporous is in agreement with the hypothesis of signal amplification because of underlying selenite in the pores and with XPS results from cadmium adsorption samples.

## Conclusions

The BE of the Al 2p line (73.5–73.6 eV) was constant regardless of adsorbent. The BE of the O 1s line was constant for the oxides (530.6 eV) and slightly higher for the hydroxide (531.2) in agreement with literature values.

The measured BEs for cadmium (Cd  $3d_{5/2} = 405.2$  eV) and selenite (Se  $3d = 58.8$  eV) sorbed on aluminum oxides were in good agreement with reported values. In addition, the BE of the Se 3d line definitely corresponds to selenite and rules out the possibility of oxidation of the adsorbate to form selenate.

Estimation of cadmium surface coverages of the porous adsorbents using XPS agrees well with the hypothesis of adsorbate intraparticle diffusion followed by sorption. The measured surface coverages in the porous adsorbents were at least 2 orders of magnitude lower than expected if cadmium had precipitated on the external surface of the particles. Estimates of surface coverages from XPS measurements on corundum were in very good agreement with predictions based on total cadmium sorption. The overestimation of surface coverages in the porous materials is probably caused by contributions to the signal from deeper (than the top surface) layers.

Analysis of XPS estimates of selenite surface coverages of the oxides studied strongly favors the hypothesis of intraparticle diffusion followed by sorption as the predominant mechanism for selenite partitioning on porous transition aluminas. The agreement between XPS estimates of the surface coverage and a total surface area utilization hypothesis was very good. The surface coverage of the porous aluminas was overestimated relative to the surface coverage of corundum for the same reasons given in the discussion of cadmium results. Selenite surface coverages appear to be underestimated compared to cadmium coverages, possibly because of overlap of the Se 3d line with Al satellites at the low Se surface coverages studied.

These results provide direct spectroscopic evidence consistent with diffusion of inorganic sorbates in the internal structure of porous adsorbents followed by adsorption as the most likely mechanism of ion sorption in porous materials, under the surface coverages studied. The results have significant implications for the treatment of wastewaters and the fate of inorganic contaminants in the environment. The fact that the internal surface area is accessible to cadmium and selenite implies that large, porous, high internal surface area adsorbents could be used to treat large volumes of wastewaters; the overall process however could be limited by intraparticle (pore) diffusion. Similarly, the transport of inorganic contaminants through aquifers could be controlled by intraparticle diffusion if porous or microporous mineral phases are present.

## Acknowledgments

I am thankful to Michael F. Hochella Jr. for his overall assistance and many useful discussions and suggestions during this project. I also thank James O. Leckie for support during this study. Financial support, provided by the U.S. Environmental Protection Agency Western Region Hazardous Substance Research Center through Grant EPA-R-815738, is gratefully acknowledged. This article has not been reviewed by the U.S. Environmental Protection Agency and, therefore, does not necessarily reflect the views of this agency. The thoughtful comments and suggestions of three anonymous reviewers greatly improved the manuscript and are also acknowledged.

## Literature Cited

- (1) Davis, J. A.; Hayes, K. F. In *Geochemical Processes at Mineral Surfaces*; Davis, J. A., Hayes, K. F., Eds.; ACS Symposium Series 323; American Chemical Society: Washington, DC, 1986; pp 2–18.

- (2) Hao, O. J.; Huang, C. P. *J. Environ. Eng. Div. ASCE* **1986**, *112*, 1054–1069.
- (3) Batchelor, B.; Dennis, R. J. *Water Pollut. Control Fed.* **1987**, *59*, 1059–1068.
- (4) Bottero, J. Y.; Thomas, F.; Leprince, A. *Aqua* **1983**, *2*, 69–73.
- (5) Chen, A. S. C.; Snoeyink, V. L.; Mallevalle, J.; Fiessinger, F. *J. Am. Water Works Assoc.* **1989**, *81*, 53–60.
- (6) Chen, A. S. C.; Snoeyink, V. L.; Fiesinger, F. *Environ. Sci. Technol.* **1987**, *21*, 83–90.
- (7) Thomas, F.; Bottero, J. Y.; Cases, J. M. *Colloids Surf.* **1989**, *37*, 269–280.
- (8) Thomas, F.; Bottero, J. Y.; Cases, J. M. *Colloids Surf.* **1989**, *37*, 281–294.
- (9) Papelis, C. Ph.D. Dissertation, Stanford University, Stanford, CA, 1992.
- (10) Papelis, C.; Roberts, P. V.; Leckie, J. O. *Environ. Sci. Technol.* **1995**, *29*, 1099–1108.
- (11) Sposito, G. In *Geochemical Processes at Mineral Surfaces*; Davis, J. A., Hayes, K. F., Eds.; ACS Symposium Series 323; American Chemical Society: Washington, DC, 1986; pp 217–228.
- (12) Briggs, D., Seah, M. P., Eds. *Practical Surface Analysis, Volume 1, Auger and X-ray Photoelectron Spectroscopy*, 2nd ed.; John Wiley & Sons: New York, 1990; p 657.
- (13) Hochella, M. F., Jr.; Carim, A. H. *Surf. Sci.* **1988**, *197*, L260–L268.
- (14) Stipp, S. L.; Hochella, M. F., Jr. *Geochim. Cosmochim. Acta* **1991**, *55*, 1723–1736.
- (15) Hochella, M. F., Jr. In *Mineral-Water Interface Geochemistry*; Hochella, M. F., Jr., White, A. F., Eds.; Reviews in Mineralogy; Mineralogical Society of America: Washington, DC, 1990; pp 87–132.
- (16) Kelly, M. A. In *Encyclopedia of Materials Science and Engineering*; Bever, M. B., Ed.; Pergamon Press: Oxford, 1986; pp 1462–1467.
- (17) Perry, D. L.; Taylor, J. A.; Wagner, C. D. In *Instrumental Surface Analysis of Geologic Materials*; Perry, D. L., Ed.; VCH Publishers: New York, 1990; pp 45–86.
- (18) Hochella, M. F., Jr. In *Spectroscopic Methods in Mineralogy and Geology*; Hawthorne, F. C., Ed.; Reviews in Mineralogy; Mineralogical Society of America: Washington, DC, 1988; pp 573–637.
- (19) Brundle, C. R.; Baker, A. D., Eds. *Electron Spectroscopy: Theory, Techniques and Applications*; Academic Press: London, 1978; p 287.
- (20) Scofield, J. H. *J. Electron Spectrosc. Relat. Phenom.* **1976**, *8*, 129–137.
- (21) Swift, P. *Surf. Interface Anal.* **1982**, *4*, 47–51.
- (22) Seah, M. P.; Swift, P.; Shuttleworth, D. In *Practical Surface Analysis Volume 1, Auger and X-ray Photoelectron Spectroscopy*; Briggs, D., Seah, M. P., Eds.; John Wiley & Sons: New York, 1990; pp 541–554.
- (23) Bertoti, I.; Mink, G.; Varsanyi, G.; Szekeley, T. *Vacuum* **1987**, *37*, 141–143.
- (24) Grunert, W.; Shpiro, E. S.; Feldhaus, R.; Anders, K.; Antoshin, G. V.; Minachev, K. M. *J. Catal.* **1987**, *107*, 522–534.
- (25) Kasztelan, S.; Grimblot, J.; Bonnelle, J. P.; Payen, E.; Toulhoat, H.; Jacquin, Y. *Appl. Catal.* **1983**, *7*, 91–112.
- (26) Kaushik, V. K.; Sivaraj, C.; Rao, P. K. *Appl. Surf. Sci.* **1991**, *51*, 27–33.
- (27) Madey, T. E.; Wagner, C. D.; Joshi, A. *J. Electron Spectrosc. Relat. Phenom.* **1977**, *10*, 359–388.
- (28) Stranick, M. A.; Houalla, M.; Hercules, D. M. *J. Catal.* **1987**, *106*, 362–368.
- (29) Strohmeier, B. R.; Hercules, D. M. *J. Phys. Chem.* **1984**, *88*, 4922–4929.
- (30) Strohmeier, B. R.; Hercules, D. M. *J. Catal.* **1984**, *86*, 266–279.
- (31) Strohmeier, B. R.; Leyden, D. E.; Field, R. S.; Hercules, D. M. *J. Catal.* **1985**, *94*, 514–530.
- (32) Strohmeier, B. R.; Evans, W. T.; Schrall, D. M. *J. Mater. Sci.* **1993**, *28*, 1563–1572.
- (33) Tan, B. J.; Klabunde, K. J.; Sherwood, P. M. A. *J. Am. Chem. Soc.* **1991**, *113*, 855–861.
- (34) Rebenstorff, B.; Lars, S.; Andersson, T. *J. Chem. Soc. Faraday Trans.* **1990**, *86*, 3153–3158.
- (35) Bonnelle, J. P.; Grimblot, J.; D'Huysser, A. *J. Electron Spectrosc. Relat. Phenom.* **1975**, *7*, 151–162.
- (36) Fritsch, A.; Legare, P. *Surf. Sci.* **1987**, *184*, L355–L360.
- (37) Lindsay, J. R.; Rose, H. J., Jr.; Swartz, W. E., Jr.; Watts, P. H., Jr.; Rayburn, K. A. *Appl. Spectrosc.* **1973**, *27*, 1–5.
- (38) Majumdar, D.; Chatterjee, D.; Ghosh, S.; Blanton, T. *Appl. Surf. Sci.* **1993**, *68*, 189–195.
- (39) McGuire, G. E.; Schweitzer, G. K.; Carlson, T. A. *Inorg. Chem.* **1973**, *12*, 2450–2453.
- (40) McIntyre, N. S.; Cook, M. G. *Anal. Chem.* **1975**, *47*, 2208–2213.
- (41) Nefedov, V. I.; Gati, D.; Dzhurinskii, B. F.; Sergushin, N. P.; Salyn, Y. V. *Russ. J. Inorg. Chem.* **1975**, *20*, 1279–1283.
- (42) Nefedov, V. I.; Salyn, Y. V.; Leonhardt, G.; Scheibe, R. *J. Electron Spectrosc. Relat. Phenom.* **1977**, *10*, 121–124.
- (43) Ng, K. T.; Hercules, D. M. *J. Phys. Chem.* **1976**, *80*, 2094–2102.
- (44) Ogilvie, J. L.; Wolberg, A. *Appl. Spectrosc.* **1972**, *26*, 401–403.
- (45) Paparazzo, E. *Appl. Surf. Sci.* **1986**, *25*, 1–12.
- (46) Paparazzo, E. *J. Electron Spectrosc. Relat. Phenom.* **1987**, *43*, 97–112.
- (47) Patterson, T. A.; Carver, J. C.; Leyden, D. E.; Hercules, D. M. *J. Phys. Chem.* **1976**, *80*, 1700–1708.
- (48) Wagner, C. D.; Passoja, D. E.; Hillery, H. F.; Kinisky, T. G.; Six, H. A.; Jansen, W. T.; Taylor, J. A. *J. Vac. Sci. Technol.* **1982**, *21*, 933–944.
- (49) Moulder, J. F.; Stickle, W. F.; Sobol, P. E.; Bomben, K. D. *Handbook of X-ray Photoelectron Spectroscopy*; Perkin-Elmer Corp., Physical Electronics Division: Eden Prairie, MN, 1992; p 261.
- (50) Papelis, C.; Brown, G. E., Jr.; Parks, G. A.; Leckie, J. O. *Langmuir*, in press.
- (51) Klauber, C.; Smart, R. S. C. In *Surface Analysis Methods in Materials Science*; O'Connor, D. J., Sexton, B. A., Smart, R. S. C., Eds.; Springer Series in Surface Sciences 23; Springer-Verlag: Berlin, 1992; pp 3–65.
- (52) Cotton, F. A.; Wilkinson, G. *Advanced Inorganic Chemistry, a Comprehensive Text*; John Wiley & Sons: New York, 1980; p 1396.
- (53) Hayes, K. F.; Papelis, C.; Leckie, J. O. *J. Colloid Interface Sci.* **1988**, *125*, 717–726.
- (54) Gregg, S. J.; Sing, K. S. W. *Adsorption, Surface Area and Porosity*; Academic Press Inc.: London, 1982; p 303.
- (55) White, A. F.; Peterson, M. L. In *Chemical Modeling of Aqueous Systems II*; Melchior, D. C., Bassett, R. L., Eds.; ACS Symposium Series 416; American Chemical Society: Washington, DC, 1990; pp 461–475.

Received for review August 23, 1994. Revised manuscript received December 30, 1994. Accepted March 7, 1995.\*

ES9405383

\* Abstract published in *Advance ACS Abstracts*, April 15, 1995.